



USING A MULTILATERATION STRATEGY TO DETERMINE THE SENSOR POSITIONS IN ACOUSTIC ARRAY MEASUREMENTS

Ingo B. Witew

Michael Vorländer

Institute of Hearing Technology and Acoustics, RWTH Aachen University, Germany

ABSTRACT

In acoustic array applications, it is important to know the sensor positions as precisely as possible in order to reduce the residual terms in the subsequent data processing. Depending on the mechanical design, especially with larger setups, the situation can arise, that the actually reached sensor positions are uncertain. In this contribution array measurements to sample the sound field in auditoria over an area of 8m x 5.3m are presented. A special focus is placed on the discussion how the measurement locations can be determined as accurately as possible. Several secondary loudspeakers were installed in the array, which allow surveying the direct sound propagation in the setup. Using an acoustic multilateration approach on this data, the positions of the sensors can be determined. A special feature of this quasi-blind approach is that the input data for the multilateration can be uncertain. The uncertainty of the so identified measurement locations is evaluated and the relevance for the subsequent data processing is discussed.

Keywords: Array measurements, Measurement uncertainty, Multilateration

1. INTRODUCTION

The microphone location is an important factor in room acoustical measurements for a number of reasons. In clas-

*Corresponding author: Ingo.Witew@akustik.rwth-aachen.de.

Copyright: ©2023 Witew et al. This is an open-access article distributed under the terms of the Creative Commons Attribution 3.0 Unported License, which permits unrestricted use, distribution, and reproduction in any medium, provided the original author and source are credited.

sical (ISO3382) measurements it is a key factor to enable reproducible measurements which require properly defined source and receiver locations. In array measurements the data analysis requires precise knowledge of the (relative) sensor positions, too, as phase differences between the sensors are regularly analyzed.

In practical room acoustical measurements there are some challenges that make it difficult to determine the sensor positions. Auditoria are relatively large and oftentimes feature room shapes that included raked audience areas or curved surfaces which makes it difficult and thus uncertain to survey the Cartesian coordinates of a location. Frequently, positions are given relative to reference objects (e.g. seat A in row B) whose position is not available in Cartesian coordinates when high quality architectural drawings are not available. With optimized measurement procedures it is within reach to survey a large number of receiver positions through repeated measurements. The already high effort to precisely determine measurement positions is thus multiplied.

In array measurements, the used strategies are very versatile. When sensor locations are very numerous, robotic setups are occasionally utilized to automatically position the microphones during series of repeated measurements, e.g. [1], [2], [3] or [4]. Depending on the detailed strategy employed, the question may arise as to how precisely the intended sensor position was reached by the robot.

Against this background it is reasonable to discuss a method that determines the actually sampled location in acoustic array measurements. Without loss of generality the example of a measurement robot developed at IHTA is used to discuss how microphone positions were determined acoustically using a multilateration method.



2. METHODOLOGY

2.1 Background - Measurement scenario

In order to study the uncertainty of room acoustical measurements the measurement setup shown in Figure 1 was designed that allows sampling the sound field in auditoria over an area of $8\text{ m} \times 5.3\text{ m}$ at any resolution. An aluminum frame structure holds three rails that carries a movable carbon truss. 32 microphones are mounted to this truss at a distance of 25 cm. Using carbon tubes the microphones are lowered to the sampling surface at about 1.2 m above the auditorium's floor. Through motorized actuators the truss can be moved over an area of $0.25\text{ m} \times 5.3\text{ m}$ thus yielding a combined area of $8\text{ m} \times 5.3\text{ m}$ that can be surveyed by the 32 microphones. In pursued measurement surveys a Cartesian resolution of 5 cm was implemented leading to array measurements with a total of 16 960 sampling locations. A detailed review of the measurement device can be found at [4].

Due to a combination of design decisions and manufacturing tolerances, it is not ensured that the intended microphone positions are reached with ultimate accuracy. This leads to the wish to determine the actually achieved measurement position and use it for further analysis. Out of an affinity to acoustical solutions, and since electromagnetic tracking methods for all 32 microphones did not represent a feasible strategy, an acoustical multilateration method was chosen to determine the actual microphone position during the room acoustical measurements. As marked in Figures 1 and 2 through red circles, a total of six small loudspeakers were mounted in the aluminum frame of the measurement array. These secondary sound sources permit measuring $6 \times 16\ 960$ impulse responses to determine the direct sound's "time of flight" between the small loudspeakers and each of the microphones. Measurements with the small loudspeakers were conducted using swept sine signals of the FFT degree 15 without averages and a sampling rate of 44.1 kHz. After deconvolution the derived impulse responses covered the 1–8 kHz octave bands and featured a peak/noise ratio of approximately 50 dB.

2.2 Background - Multilateration

The first application of multilateration (in combination with triangulation) can be traced back to the 1910s. Reportedly this technology was developed independently by the Russians, Germans, French, Americans and very successfully by the British to detect hostile artillery during

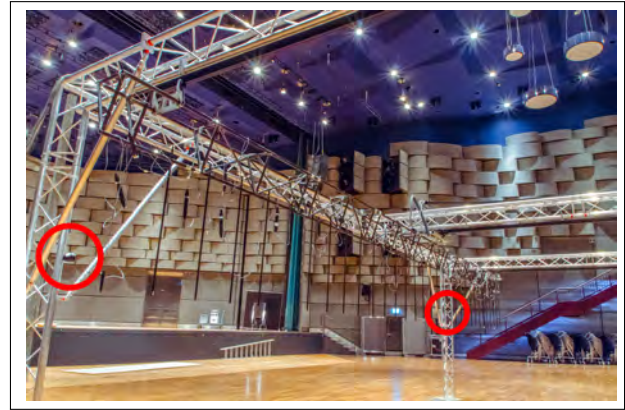


Figure 1. Detailed view of small loudspeakers mounted in the measurement setup's frame structure.

World War I. From the time delay of the firing boom between two microphones, the bearing to firing sites was determined. The most common present day applications of multilateration are the *NAVSTAR* or the *Galileo* global positioning systems. The topic is widely investigated with a large number of different approaches and dialects. As an example, three investigations from the same year can be cited: [5] describe a procedure based on intersecting hyperboloids, [6] publishes about the application of the PHAT algorithm and [7] report on a closed-form least-squares solution. Acoustical applications cover a wide range as well, including the detection of aircraft and submerged vehicles [8], video camera steering [9] or animal bioacoustics [10].

Against the background of the numerous research activities and the technical maturity of the applications, it is not obvious whether and how an innovation could be developed without long experience in this particular field of research. At the time of implementation, however, literature review gave no indication that such strategies had previously been implemented as (quasi) blind methods (i.e., without exact knowledge of the sensor positions) or in room acoustical applications.

2.3 Implementation

The principle of multilateration is based on the measurement of a wave's arrival times at a number of sensors under the assumption that the wave's propagation speed is constant, that the clocks at the receivers are synchronized and that the path between the source and the receiver is direct, i.e. unobstructed. In the case discussed here, the

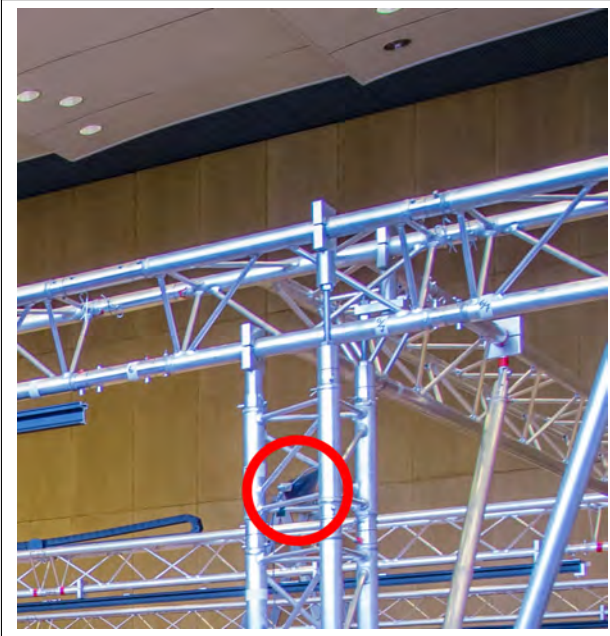


Figure 2. Detailed view of small loudspeakers mounted in the measurement setup's frame structure.

measured data can be interpreted after the deconvolution as if the small distributed loudspeakers had emitted an impulse in their own respective measurements. Due to the (constant) latency of the measurement system, this impulse is delayed by t_{latency} before it propagates in a spherical wave through the medium and eventually passes the microphones at the time t_{em} . This relation is expressed in Equation 1 and is visualized in Figure 3 through the red circles.

$$t_{\text{em}} = \frac{R_{\text{em}}}{c} + t_{\text{latency}} \quad (1)$$

with

$$R_{\text{em}} = |\vec{x}_{\text{m}} - \vec{x}_{\text{e}}|_2$$

$$c = 331.3 + 0.606\vartheta.$$

R_{em} denotes the distance between the emitter at \vec{x}_{e} and the microphone at \vec{x}_{m} . c is the speed of sound as a function of temperature ϑ ([26], [25]).

Equation 1 can be set up for each combination of the six "position loudspeakers" and the 16 960 microphones. This system features 101 760 equations with 50 900 unknown variables, i.e., three position coordinates for each

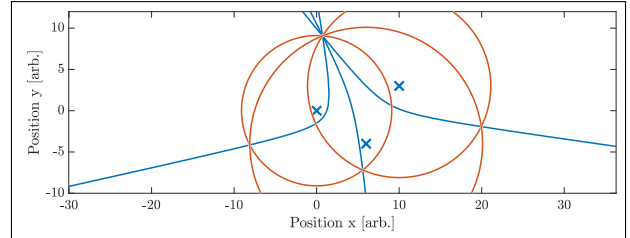


Figure 3. Comparison of time-of-arrival (red) and time-difference-of-arrival (blue) approaches to detect a source's position. The emitter positions are marked by blue X (after [12]).

of the microphones and the loudspeakers and the temperature and latency. The unknowns can be determined (see Equation 2) by a Levenberg-Marquardt nonlinear least-squares optimization approach [11].

$$\min_{\substack{|\vec{x}_{\text{m}} - \vec{x}_{\text{e}}|_2 \in \mathbb{R}^3 \setminus \vec{0} \\ t_{\text{latency}} \in \mathbb{R}^+ \\ \vartheta \in \mathbb{R} \setminus \infty}} |\vec{t}_{\text{em,measured}} - \vec{t}_{\text{em}}| \quad (2)$$

This formulation raises the problem that for $\vec{x}_{\text{m}}, \vec{x}_{\text{e}} = \vec{0}$ and $\vartheta \rightarrow \infty$, there is a singular solution that is not particularly reasonable, and that the solution space is indifferent to rotations and scaling. These challenges can, however, be avoided by choosing an iterative method through which the speaker and the microphone positions cannot be optimized at the same time. In addition, the solution space is subject to a rotation normalization by minimizing the variance of the microphone positions along the z -axis.

For a good optimization of the problem it is important to have an accurate measurement of the arrival times of the direct sound. Here, the time of arrival of the direct sound is defined as the time sample of the highest amplitude's absolute value. Alternative definitions that rely on the first rising of the signal amplitude above a pre-defined level (e.g., [13]) were not proven to be very effective, as the coincidental detection of local extrema would introduce a significant variation in the detected time-of-arrivals. Establishing the absolute maximum leads to much more accurate results, but the measured times are still uncertain by ± 0.012 ms because of the sampling rate of 44.1 kHz. What may not appear at first glance to be problematic corresponds to an uncertainty of the distance measurement of some 7 to 8 mm depending on the prevailing speed of sound. However, since the band-limited signal can be perfectly reconstructed below Nyquist and Shannon's cutoff

frequency, there is no good reason to reduce the accuracy of the optimization due to uncertain input data.

Through trial and error, it was determined that by applying up to a 100-fold upsampling to determine the time-of-arrival, the accuracy of the optimization could be improved. The upsampling results in a theoretical accuracy of $\pm 0.11 \mu\text{s} \approx \pm 39 \mu\text{m}$ for the arrival time measurement. This may be a limitation due to the clock jitter, which the manufacturer of the hardware quantifies as "less than 5 ns". In contrast to the discussion before, however, the uncertainty in the time-of-arrival measurement is very small compared to the time it takes for the sound wave to travel through the entire array. This difference in orders of magnitude constrains the uncertainty of the output to very small and potentially negligible values [14, Ch. 2].

Another aspect that is detrimental to the accurate determination of the arrival time is the false detection of reflections. Due to the high directivity of the small loudspeaker diaphragms and due to nearby surfaces, there is the occasional problem that a later reflection features a higher amplitude than the (off-axis) direct sound. In such situations, the measured arrival times are far too late. This large time difference between adjacent measurement locations and the knowledge that the earlier arrival time is the "better" time makes it relatively easy to adjust the search interval for the direct sound maximum. Figure 4 shows a particularly error-prone example in which the initial falsely detected times-of-arrival have been identified and corrected, yielding the distribution shown in Figure 5.

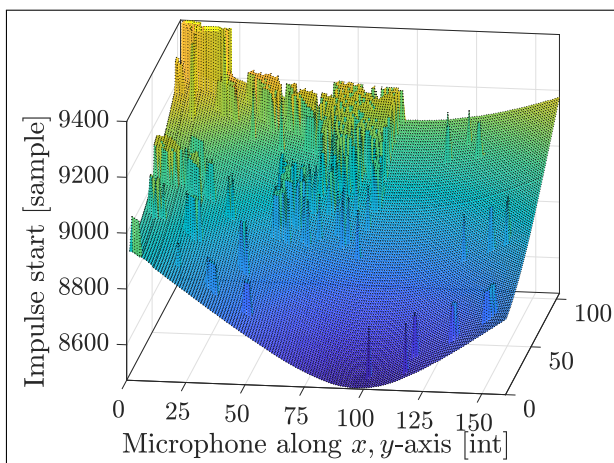


Figure 4. Detected arrival of the direct sound with outliers.

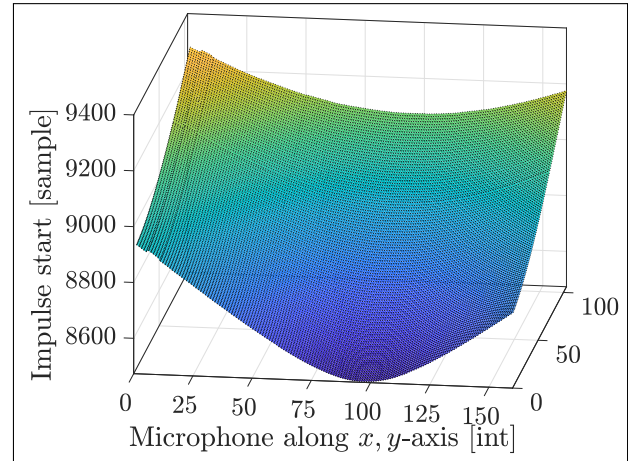


Figure 5. Corrected arrival of the direct sound.

3. RESULTS

The results of the multilateration can be seen exemplarily in Figure 6, which shows how this approach can be used to determine generally plausible microphone positions: the red dots mark the detected positions of the loudspeakers. On closer examination of the identical results shown in Figure 7, it becomes clear that the z -dimension follows a position-dependent systematic trend. Even when this wave pattern does not appear to be particularly large relative to the dimensions of the sampling area, these results fall short of the authors' initial expectations.

3.1 Accuracy of the estimation

Considering the working principle of the measurement robot, the wide range in z -coordinates shown in Figure 7 feeds the suspicion that not all positions were estimated with the same accuracy. On the assumption that iid normality of the involved uncertainty distributions can be maintained, [15] present a strategy that permits quantifying the confidence region of a nonlinear optimization's result (i.e., the determined microphone positions) based on the equation system's Jacobian matrix. Considering that the Jacobian is the first-order partial derivative of a vector-valued function [16, 12.8.2], the analogies to the multi-dimensional standard GUM method become obvious. This analogy helps in the intuitive understanding of the method. The residual after optimization is divided equally among the input variables and is understood as their uncertainty. Corresponding to the uncertainty propagation, the Jacobi matrix indicates how input uncertain-

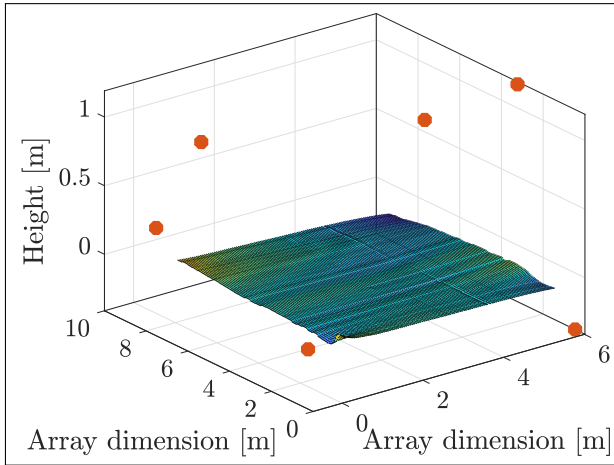


Figure 6. Multilateration results: Microphone and loudspeaker positions. Overview with loudspeakers (red).

ties are reduced to output uncertainties. Consequently, the normality prerequisite of the [15] method coincides with the fundamental assumption of this investigation and the GUM framework, and can be justified on the grounds of the central limit theorem.

The uncertainties of the determined microphone positions (as the ℓ^2 -norm) are shown in Figure 8 through the color of the position markers. In addition, the uncertainty histogram plotted in Figure 9 permits a second perspective. These images show two aspects: First, the initial suspicion that the wave pattern in Figure 7 is a (general) indication of estimation's uncertainty is confirmed by Figure 9. Second, it can be seen that standard uncertainties of up to 40 cm can hardly be interpreted as sufficient for many applications.

4. REVISED METHODOLOGY

These results support the wish to modify the optimization strategy to increase accuracy. The design of the measurement setup features a carbon truss from which the 32 microphones are lowered on rigid carbon tubes. This implies that each of the microphones may have individual elevations (z -coordinates): however, along the path each microphone travels, all of the respective 530 measurement positions must have the same z -coordinate. This reduces the degrees of freedom from 50 900 to only 33 972. By exploiting this additional boundary condition, the underlying system of equations is significantly better conditioned,

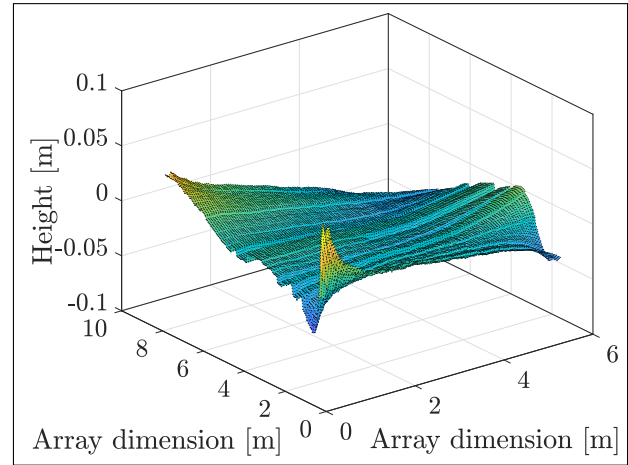


Figure 7. Multilateration results: Microphone and loudspeaker positions. Detailed view with expanded z -axis.

and thus yields much smaller uncertainties.

5. RESULTS

For the same data the uncertainty of the microphone positions based on the revised conditions are shown in Figures 10 and 11. The confidence intervals are now more evenly distributed over the sampling areas that the different physical microphones cover. Additionally, the color coding and the histogram data give evidence that the standard uncertainty has been significantly reduced to less than 1 cm. Changes of several orders of magnitude are no longer very easy to display graphically on a linear scale; therefore, the color scaling has been changed by a factor of 50 when comparing Figures 8 and 10.

6. VALIDATION

Since it is not automatically guaranteed that overdetermined optimization problems converge towards the absolute minimum when they are solved, an independent validation is appropriate. Measurements conducted in an auditorium with variable acoustics provide the data for such a validation as setup was used repeatedly in immediate succession for seven times. While different acoustic setups of the room were studied the setup of the measurement device was not altered, i.e., neither the loudspeaker positions nor the z -coordinates of the 32 microphones were changed. This offers the opportunity to deter-

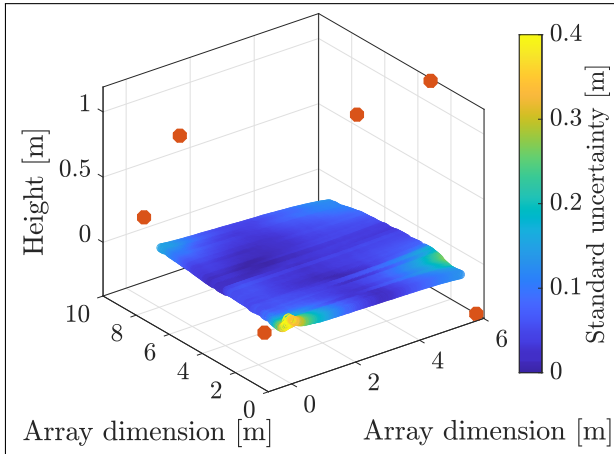


Figure 8. Uncertainty of the detected microphone positions. Spatial distribution.

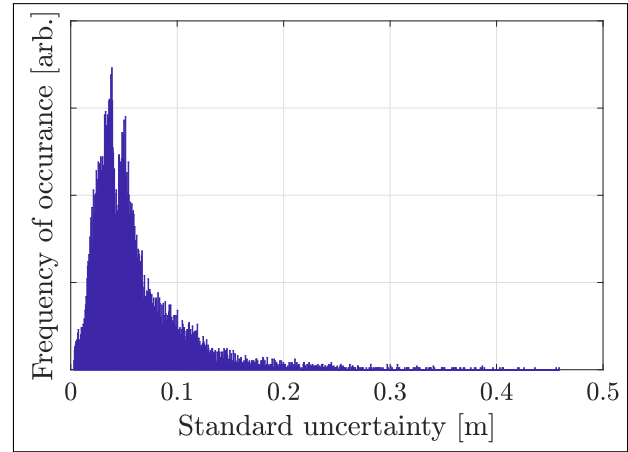


Figure 9. Uncertainty of the detected microphone positions. Uncertainty histogram.

mine whether the independently determined microphone and loudspeaker positions are comparable.

Figure 12 shows in blue the empiric standard deviation of the seven determined z -coordinates for each of the 32 microphones. As a comparison, the average over seven 68 % confidence intervals based on [15] is displayed in red. The z -coordinates from the 7 multilaterations exhibit a standard uncertainty of about 0.51 mm, whereas [15]’s algorithm predicts an average standard uncertainty of 0.37 mm.

7. DISCUSSION

With the approach described here, a best estimate of the relative measurement position can be determined along with its uncertainty. In acoustics, the proposed accuracy seems almost unheard of and absurd, since it is already on the order of magnitude of the microphone’s capsule and membrane, and even the acoustic wavelength. The latter aspect in particular should encourage caution in considering such (low) uncertainties. It is probably due to the three-fold overdetermination of the system of equations, and the associated averaging effects, that the measurement locations can be determined so precisely when wave effects would not initially support this.

Estimating the confidence intervals of the results is based on the assumption that iid normality can be assumed for all optimization variables in Equation 1 and 2. Of the 33972 variables, 33952 are position coordinates of the microphones and 18 variables correspond to the po-

sitions of the loudspeakers. The two remaining variables are the air temperature and measurement systems latency. In a strict interpretation it seems clear that this mixture of variables is unlikely to have similar stochastic properties. In a more practical approach, however, it is evident that the vast majority of optimization variables are microphone position coordinates and it is plausible that they have similar properties. The basic assumption that the optimization variables are independent draws from similar distributions seems defensible in this context.

The strategy used is based on the assumption of unobstructed direct sound propagation between source and receiver. For the application discussed here, i.e. that of determining the microphone positions in room acoustic measurements in auditoria, in common geometries this condition is often easily fulfilled on its own or by careful placement of the secondary sources. However, theoretic measurement setups are conceivable, for instance to survey acoustically coupled volumes where unobstructed propagation of the direct sound is not a given. In such scenarios, the setup or the strategy would have to be suitably adapted.

In the strategy presented here, evidence emerged that the directivity of the secondary sources complicated the detection of the direct sound. Although an effective method was presented for overcoming this challenge, other strategies that detect the impulse launch by other means are also conceivable, e.g. [23], [24]. Comparing the effectiveness of the different methods can be undertaken in a separate study.

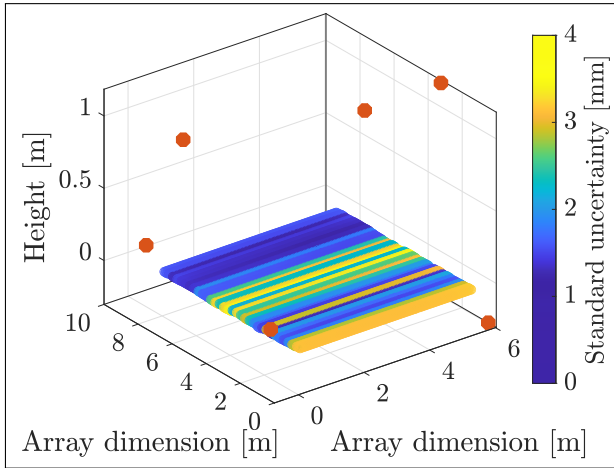


Figure 10. Uncertainty of the detected microphone positions for the revised optimization approach. Compared to Figure 8, the color coded display range has been reduced by a factor of 100. Spatial distribution.

The analysis presented here is based on the assumption that sound propagation is unchanged over the duration of the measurement. Strictly speaking, however, the speed of sound changes due to inevitable changes in air temperature during the measurement. With the relatively short distances between source and receiver occurring here, and with the small changes in temperature documented before and after the series of measurements within 1 K, the influence is relatively small. However, it is recognized that the influence of a change in temperature can be more pronounced. Therefore it is supported by the problems degrees of freedom to discuss this influence in more detail in a future study, in which the temperature is taken into account as a time-varying optimization variable. This influence on the accuracy of the estimation can then be considered more precisely.

Finally, the question arises whether the so determined microphone positions are suitable for a further evaluation. The answer to this question depends, of course, on the intended type of further processing and on the discussed frequency and wavelength. In this particular case the collected data was used to investigate the influence of the measurement position on room acoustical measurements. In this context it is relevant that the sampling locations can be determined with an accuracy that is significantly higher than that of the sampling grid (i.e. 5 cm), and

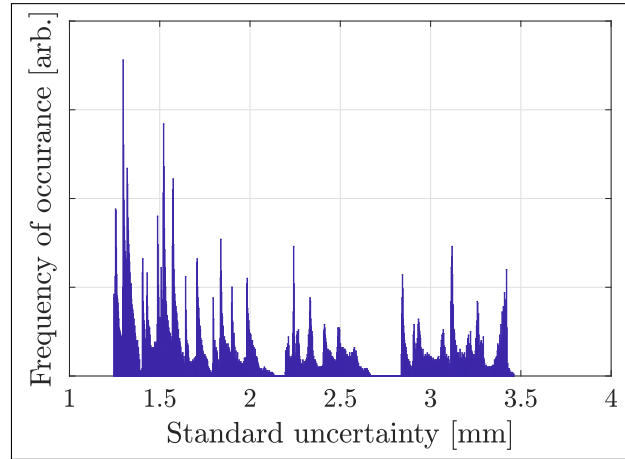


Figure 11. Uncertainty of the detected microphone positions for the revised optimization approach. Compared to Figure 9, the color coded display range has been reduced by a factor of 100. Uncertainty histogram.

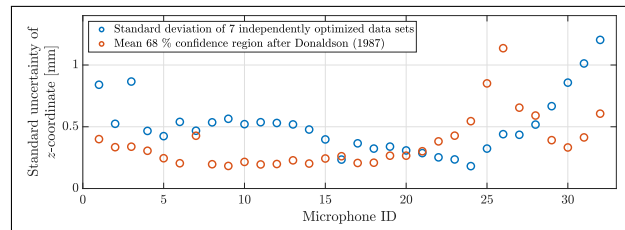


Figure 12. Comparison of different methods to determine the uncertainty of the multilateration.

also more accurately than the underlying driving forces, i.e., decorrelation of the sound field over space of about $\sin(ka)/ka$ [17]. Compared to other investigations (e.g., [18], [19], [20], [21], and others), where measurement positions are given relative to reference objects such as numbered seats, the accuracy determined here appears absolutely adequate. Whether the determined uncertainties are sufficient for array applications, for which the phase of the microphone signals is crucial, has to be investigated in a separate study.

8. CONCLUDING REMARKS

This contribution reports on the application of a multilateration approach to acoustically determine the position of

array microphones in room acoustic measurements. Measurement positions have been established with an uncertainty of a few millimeters. This accuracy is adequate for ISO3382-measurements of the acoustic conditions in auditoria. Further refining of the method should be possible.

9. ACKNOWLEDGEMENTS

This manuscript was published in a similar form as part of [22].

10. REFERENCES

- [1] Nolan, M.; Verburg, S. A.; Brunskog, J. and Fernandez-Grande, E.; Experimental characterization of the sound field in a reverberation room. *J. Acoust. Soc. Am.*, 145(4), p. 2237–2246, 2019.
- [2] Götz, G.; Martinez Ornelas, A.; Schlecht, S. and Pulkki, V., Autonomous robot twin system for room acoustic measurements. *JAES*, 69(4), p. 261–272, 2021.
- [3] Xiang, N.; Alamuru, A.; Witew, I. B. and Vorländer, M., Experimental investigations on sound energy propagation in acoustically coupled volumes using a high-spatial resolution scanning system. *J. Acoust. Soc. Am.*, 143(6), p. EL437–EL442, 2018.
- [4] Witew, I. B.; Vorländer, M. and Xiang, N., Sampling the sound field in auditoria using large natural-scale array measurements. *J. Acoust. Soc. Am.*, 141(3), p. EL300–EL306, 2017.
- [5] Schau, H. and Robinson, A., Passive source localization employing intersecting spherical surfaces from time-of-arrival differences. *IEEE Transactions on Acoustics, Speech, and Signal Processing*, 35(8), p. 1223–1225, 1987.
- [6] Carter, G. C., Coherence and time delay estimation. *Proc. IEEE*, 75(2), p. 236–255, 1987.
- [7] Smith, J. and Abel, J., Closed-form least-squares source location estimation from range-difference measurements. *IEEE Transactions on Acoustics, Speech, and Signal Processing*, 35(12), p. 1661–1669, 1987.
- [8] Torrieri, D. J., Statistical Theory of Passive Location Systems. *IEEE Transactions on Aerospace and Electronic Systems*, AES-20(2), p. 183–198, 1984.
- [9] Huang, Y.; Benesty, J. and Elko, G. W., Passive acoustic source localization for video camera steering. *Proc. IEEE Int. Conf. on Acoustics, Speech, and Signal Processing (Cat. No.00CH37100)*, 2, p. II909-II912, 2000.
- [10] Militello, C. and Buenafuente, S. R., An exact non-iterative linear method for locating sources based on measuring receiver arrival times. *J. Acoust. Soc. Am.*, 121(6), p. 3595–3601, 2007.
- [11] Marquardt, D. W., An Algorithm for Least-Squares Estimation of Nonlinear Parameters. *J. Soc. Ind. Appl. Math.*, 11(2), p. 431–441, 1963.
- [12] Kaune, R., Accuracy studies for TDOA and TOA localization. *Proc. Int. Conf. on Information Fusion*, 15, p. 408–415, 2012.
- [13] ISO 3382-1, Acoustics – Measurement of room acoustic parameters – Part 1: Performance spaces. International Organization for Standardization, Geneva, Switzerland, 2009.
- [14] Carroll, R. J.; Ruppert, D.; Stefanski, L. A. and Crainiceanu, C. M., *Measurement Error in Nonlinear Models – A Modern Perspective*. Chapman and Hall / CRC Press, 2nd edition, Boca Raton, USA, 2006.
- [15] Donaldson, J. R. and Schnabel, R. B., Computational Experience with Confidence Regions and Confidence Intervals for Nonlinear Least Squares. *Technometrics*, 29(1), p. 67–82, 1987.
- [16] Bronstein, I. N.; Semendyayev, K. A.; Musiol, G. and Mühlig, H., *Handbook of Mathematics*. Springer, 6th edition, Berlin, Heidelberg, Germany, 2015.
- [17] Bodlund, K., A normal mode analysis of the sound power injection in reverberation chambers at low frequencies and the effects of some response averaging methods. *J. Sound and Vibration*, 55(4), p. 563–590, 1977.
- [18] Akama, T.; Suzuki, H. and Omoto, A., Distribution of selected monaural acoustical parameters in concert halls. *Applied Acoustics*, 71(2), p. 564–577, 2010.
- [19] Barron, M., Impulse testing techniques for auditoria. *Applied Acoustics*, 17(3), p. 165–181, 1984.
- [20] Bradley, J. S., An international comparison of room acoustic measurement systems. *IRC Internal Report*, 714(1), p. 1-130, 1996.
- [21] Lokki, T., Throw Away That Standard and Listen: Your Two Ears Work Better. *Building Acoustics*, 20(4), p. 283–293, 2013.
- [22] Witew, I., *Measurements in room acoustics - Uncertainties and influence of the measurement position*. Dissertation RWTH Aachen University, Logos Verlag, Berlin, Germany, 2022, DOI: 10.18154/RWTH-2022-08992.
- [23] Defrance, G.; Daudet, L. and Polack, J.-D. Finding the onset of a room impulse response: Straightforward? *J. Acoust. Soc. Am.*, 124, EL248–EL254, 2008.
- [24] Usher, J. An improved method to determine the onset timings of reflections in an acoustic impulse response. *J. Acoust. Soc. Am.*, 127, EL172–EL177, 2010.
- [25] Bohn, D. A. Environmental effects on the speed of sound. *JAES*, 36(4), 223–231, 1988
- [26] Rossing, T. D. Chapter 2 - A Brief History of Acoustics. In T. D. Rossing(Ed.), *Handbook of Acoustics* (pp. 9–24). New York, NY: Springer, 2007.